

# Recycling of tilapia carcass waste to obtain nanostructured biphasic calcium phosphate powder

T. H. A. Corrêa<sup>1</sup>, J. N. F. Holanda<sup>1\*</sup>

<sup>1</sup>State University of Northern Fluminense Darcy Ribeiro, Laboratory of Advanced Materials, Group of Ceramic Materials, Campos dos Goytacazes, RJ, Brazil

## Abstract

In Brazil, a significant amount of tilapia carcass waste is produced every year. The aim of this study is to evaluate the recycling of tilapia carcass waste as an alternative calcium precursor to produce biphasic calcium phosphate (BCP) powder via a wet chemical precipitation method in different  $\text{HNO}_3$  concentrations. The synthesized powders were characterized by X-ray diffraction, scanning electron microscopy, thermogravimetric analysis, Fourier transform infrared spectroscopy, average crystallite size, and refinement by the Rietveld method for the quantification of crystalline phases. The experimental results indicated the formation of a BCP bioceramic with different amounts of  $\beta$ -calcium pyrophosphate ( $\beta$ -CPP) and  $\beta$ -tricalcium phosphate ( $\beta$ -TCP), depending on the  $\text{HNO}_3$  concentration. The new BCP powders showed an average crystallite size between 57.7 and 59.2 nm. Such a result suggests a possibility of friendly recycling of tilapia carcass waste for biomedical applications.

**Keywords:** tilapia carcass waste, biphasic calcium phosphate, nanopowders, recycling.

## INTRODUCTION

Fish is a widely consumed food worldwide because it is an important source of proteins, and vitamins, tasty and healthy for human consumption [1]. Brazil has a relevant fish processing industry distributed in all its geographic regions, with great economic and social repercussions. In 2022, Brazil produced about 860,355 tons of fish, 63.93% corresponding to Nile tilapia (*Oreochromis niloticus*) [2]. However, the filleting process of Nile tilapia generates large amounts of waste, including solid waste called the carcass (the skeleton with remnants of attached meat). Henceforth, such solid waste will be called tilapia carcass waste. A matter of great importance is its disposal without any treatment, which causes serious environmental and public health problems [3, 4]. In this context, it has become mandatory for the Brazilian fish processing industry to carry out eco-friendly management for the disposal of tilapia carcass waste generated on a large scale every year.

Calcium phosphates (CP) are widely used as ceramic biomaterials with great repercussions in medical applications, mainly in the field of bone regeneration [5-7]. Such calcium phosphate bioceramics can be essentially classified in terms of calcium (Ca) and phosphorus (P) at different molar ratios (Ca/P) ranging from 0.5 to 2.0. For example, this class of bioceramics includes calcium pyrophosphate (CPP, Ca/P=1.0),  $\alpha$ -tricalcium phosphate ( $\alpha$ -TCP, Ca/P=1.5),  $\beta$ -tricalcium phosphate ( $\beta$ -TCP, Ca/P=1.5), and hydroxyapatite (HAp, Ca/P=1.67) [7, 8]. It is noteworthy that, among all calcium

phosphate bioceramics, hydroxyapatite is the one that has been most studied considering its practical application in the biomedical area. Despite its importance, hydroxyapatite also has limitations when used in biomedical applications [9]. Due to this situation, in recent years, the development of other types of calcium phosphate bioceramics with significant advantages over pure hydroxyapatite (HAp), such as biphasic calcium phosphate (BCP) and multiphase calcium phosphate (MCP), has been increasingly encouraged. In this scenario, the BCP compositions that have received the most attention so far are HAp+ $\beta$ -TCP, HAp+ $\alpha$ -TCP, and  $\alpha$ -TCP+ $\beta$ -TCP [10-13].

It is well known that the use of polluting solid wastes as sources of alternative raw materials in the development of calcium phosphate bioceramics has increasingly attracted the interest of researchers worldwide [14]. This is a relevant approach with beneficial repercussions in terms of the circular economy and environmental sustainability, but it is also a great opportunity to add value to solid waste. From this perspective, works reported in the literature [15-20] have already demonstrated the valorization potential of fish carcass wastes in the production of calcium phosphate bioceramics. It is noteworthy that the conversion of fish carcass waste into biphasic calcium phosphate (HAP/ $\beta$ -TCP) has also been tested with promising results [21, 22]. However, tilapia carcass waste has seldom been applied to obtain BCP bioceramics. Recently, we suggested the use of tilapia carcass waste generated by the Brazilian fish processing industry to produce a BCP bioceramic [23]. In the present work, we continue to explore the use of tilapia carcass waste with the aim of increasing knowledge about its friendly recycling as a renewable calcium precursor to produce biphasic calcium phosphate (BCP= $\beta$ -CPP/ $\beta$ -TCP mixtures) in different  $\text{HNO}_3$  concentrations.

\*holanda@uenf.br

 <https://orcid.org/0000-0001-7409-0027>

## EXPERIMENTAL

Tilapia carcass waste from Southeast Brazil (Muriaé-MG) was used as a sustainable and low-cost calcium precursor to obtain biphasic calcium phosphate bioceramic. The process for obtaining tilapia carcass waste powder is shown in Fig. 1. Firstly, the tilapia carcasses (Fig. 1a) were cleaned in running water at 70 °C to remove the meat stuck to the bone and other organic impurities. Fully cleaned tilapia carcasses are shown in Fig. 1b. Then, the tilapia carcasses were disassembled (Fig. 1c) and dried in an oven at 100 °C for 24 h (Fig. 1d). Finally, they were dry ground in a laboratory ball mill (Fig. 1e) to obtain tilapia carcass waste powder (Fig. 1f) and sieved through a 140-mesh sieve (106 μm). The tilapia carcass waste powder is essentially composed of hydrated hydroxyapatite, as shown in Fig. 2.

The biphasic calcium phosphates derived from tilapia carcass waste were synthesized by the wet precipitation method

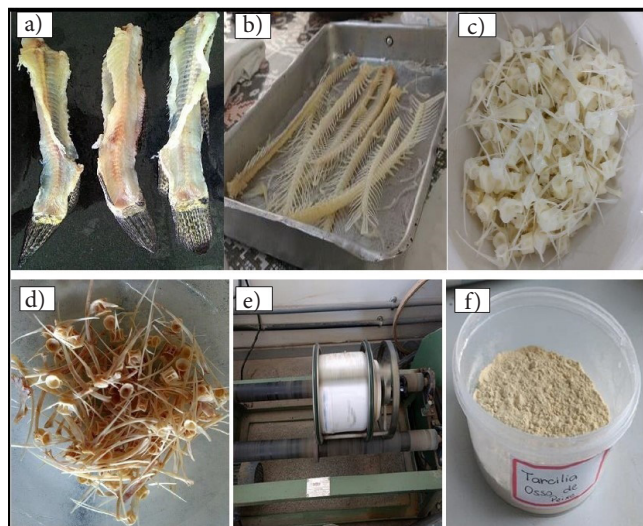


Figure 1: Images showing the production steps of the tilapia carcass waste powder: a) fresh tilapia carcass waste; b) tilapia carcass waste after cleaning; c) dismembered tilapia carcass waste; d) vertebrae from tilapia carcass waste after drying; e) grinding of the dry carcass waste in a ball mill; and f) tilapia carcass waste powder.

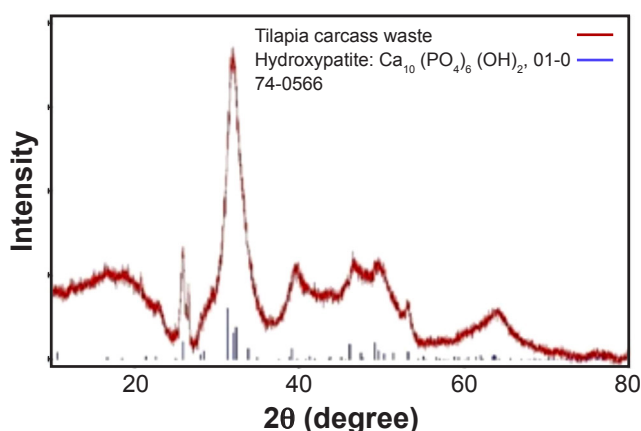


Figure 2: XRD pattern of the tilapia carcass waste powder.

[23, 24]. The commercial chemical reagents used were  $\text{HNO}_3$  (Vetec, 65%) and  $\text{Na}_2\text{HPO}_4$  (Sigma-Aldrich, 98%). Briefly, the synthesis of the biphasic calcium phosphates with a Ca/P ratio of 1.5:1 is described as follows. First, the powder from the clean tilapia carcass waste was totally dissolved in three different  $\text{HNO}_3$  solutions (1.0, 1.5, and 2.0 M) with constant stirring for 2 h, such that  $\text{Ca}(\text{NO}_3)_2$  solutions were obtained. Each sample was labeled as follows: BTC1 sample ( $\text{HNO}_3$  1.0 M); BTC2 sample ( $\text{HNO}_3$  1.5 M); and BTC3 sample ( $\text{HNO}_3$  2.0 M). Subsequently,  $\text{Na}_2\text{HPO}_4$  was dropped slowly into each  $\text{Ca}(\text{NO}_3)_2$  solution, and the solution mixtures were vigorously stirred for 2 h at 50 °C. After that, the formation of a precipitate was observed. Later, the obtained precipitates were filtered under a weak vacuum, washed with distilled water, and dried at 100 °C for 24 h. Finally, the obtained products were submitted to thermal treatment in an electrical kiln at 900 °C for 2 h and a heating rate of 10 °C/min, in order to obtain biphasic calcium phosphate powders.

The structural analysis of the as-synthesized powders was performed by X-ray diffraction (XRD) in a conventional diffractometer (Ultima IV, Rigaku) using  $\text{CuK}\alpha$  radiation over the  $2\theta=20\text{--}40^\circ$ , step size of  $0.02^\circ$ , and acquisition time of 5 s. The quantitative analysis of the crystalline phases identified in the XRD patterns was performed by refinement by the Rietveld method [25, 26]. The average crystallite sizes of the calcium phosphate bioceramics were determined based on XRD data and the Scherrer equation [27]. The morphological analysis of the synthesized powder particles was done by scanning electron microscopy (SEM, SSX-550, Shimadzu) coupled with an energy dispersive X-ray spectrometer (EDS). Thermogravimetry/derivative thermogravimetry (TG/DTG) analysis was performed using a thermal analyzer (SDT-2960, TA Instr.) in an air atmosphere at a heating rate of 10 °C/min. The Fourier transform infrared (FTIR) transmittance spectra to identify the functional groups were obtained with an FTIR spectrophotometer (Spectrum 400, Perkin-Elmer) in the range from 400 to 4000  $\text{cm}^{-1}$ .

## RESULTS AND DISCUSSION

Fig. 3 shows the XRD patterns of the calcium phosphates derived from tilapia carcass waste obtained at different  $\text{HNO}_3$  concentrations. All synthesized powders were found to provide a biphasic calcium phosphate (BCP) composed of: tetragonal structured  $\beta$ -calcium pyrophosphate [ $\beta$ -CPP,  $\beta\text{-Ca}_2\text{P}_2\text{O}_7$ ; unit cell parameters  $a=b=0.66840$  nm,  $c=0.24144$  nm, P41(76) space group; PDF file 01-071-2123], and rhombohedral structured  $\beta$ -tricalcium phosphate [ $\beta$ -TCP,  $\beta\text{-Ca}_3(\text{PO}_4)_2$ ; unit cell parameters  $a=b=0.104352$  nm and  $c=0.374029$  nm, and R3c space group; PDF 01-072-7587]. XRD patterns also indicated the presence of a majority phase corresponding to  $\beta$ -CPP. In addition, for all  $\text{HNO}_3$  concentrations, free Ca ions (PDF 01-077-7215) were also identified. This finding may be related to the increase in the pH of the calcium nitrate solution formed from the tilapia carcass waste, which releases Ca ions.

The Rietveld method was applied to refine the XRD

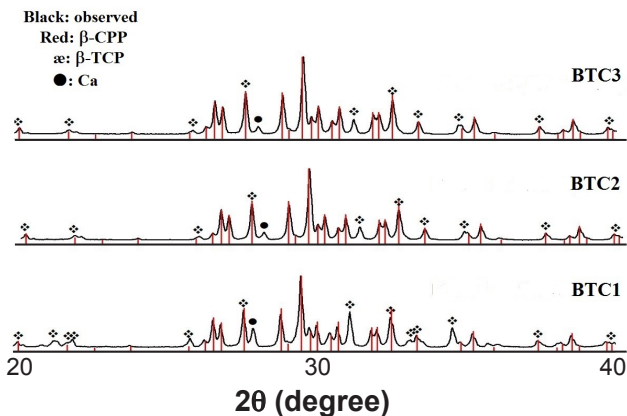


Figure 3: XRD patterns of the as-synthesized calcium phosphate powders.

data for quantitative phase determination in the synthesized calcium phosphate powders derived from tilapia carcass waste. Fig. 4 illustrates the refined XRD pattern for the BTC1 sample ( $\text{HNO}_3$  1.0 M) and the weight fractions determined after Rietveld refinement of the phase composition of all samples are provided in Table I. It appears that the obtained values for the refinement parameters ( $\chi^2=1.31-1.98$  and  $R_{wp}=10.31-15.98$ ) presented a good fit of the theoretical model to the experimental data. The BCP powders were found to have different amounts of  $\beta$ -CPP and  $\beta$ -TCP, depending on the  $\text{HNO}_3$  concentration. More specifically, the effect of increasing the concentration of  $\text{HNO}_3$  was to increase the amount of the  $\beta$ -CPP phase with concomitant decreases in the amount of the  $\beta$ -TCP phase. In addition, the amount of free Ca ions significantly decreased. These results suggested that a higher molar concentration of  $\text{HNO}_3$  (1.5 and 2.0 M) plays a decisive role in inhibiting the formation of the  $\beta$ -TCP phase. This finding is probably related to the higher acidity of the  $\text{HNO}_3$  solutions. This is in line with the results reported in the literature [24]. It is relevant to point out that the results also indicated the possibility of obtaining BCP powders with defined amounts of  $\beta$ -CPP and  $\beta$ -TCP, being adjusted simply by changing the molar concentration in the  $\text{HNO}_3$  solution. This is of the highest interest, as it makes possible the use of BCP powders for the most diverse medical applications.

Table II provides the average crystallite size of the new BCP powders derived from tilapia carcass waste, determined using the Scherrer equation. It can be seen that the increase in  $\text{HNO}_3$  concentration had little influence on the average crystallite size. In addition, the average crystallite size values between 57.7 and 59.4 nm indicated the nanostructured nature of the synthesized BCP powders. This result is of great importance, as nanostructured calcium phosphate-based bioceramics tend to favor better resorption, bioactivity, and physicochemical characteristics [28].

Fig. 5 displays SEM images of the synthesized BCP powders. It can be seen that the synthesized BCP powders had a smooth plate morphology. In these images, however, the formation of particle clusters with non-uniform sizes can also be observed. Such particle clusters with a smooth

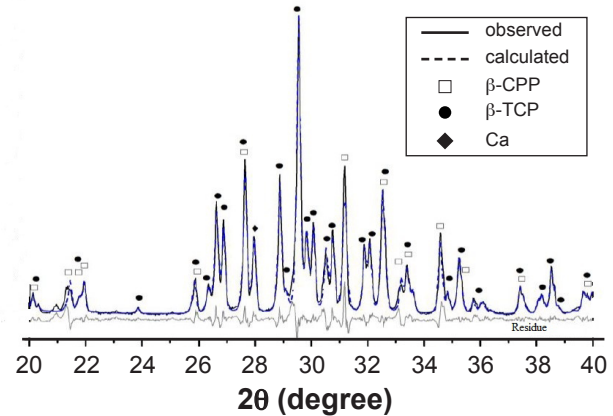


Figure 4: Rietveld refinement analysis for the XRD pattern of the BTC1 sample.

Table I - Rietveld refinement data for the synthesized calcium phosphate powders.

Sample	$\beta$ -CPP	$\beta$ -TCP	Ca	$R_{wp}$	$\chi^2$
BTC1	54.6	44.1	1.2	12.61	1.57
BTC2	94.1	5.3	0.6	10.31	1.31
BTC3	97.2	2.6	0.2	15.98	1.98

Table II - Average crystallite size (nm) of the synthesized BCP powders.

BTC1	BTC2	BTC3
59.4	57.7	59.2

surface displayed by the BCP powders derived from tilapia carcass waste are attributed to the synthesis process used, more specifically due to the calcination step at 900 °C. The Ca/P ratio values of the BCP powders were determined from the EDS analyses and are summarized in Table III. The effect of the  $\text{HNO}_3$  concentration on the Ca/P ratio was evident. The BTC1 sample had a Ca/P value of 1.56, while the BTC2 and BTC3 samples had values of 1.28 and 1.29, respectively. Such results reflect the increase in  $\text{HNO}_3$  concentration, resulting in an increase in the amount of the  $\beta$ -CPP phase in the synthesized BCP, as observed in Table I.

Fig. 6 depicts the FTIR spectra of the synthesized BCP powders. Only small differences were found between the FTIR spectra. This was related to the different amounts of the  $\beta$ -CPP and  $\beta$ -TCP phases, as shown in Table I. The frequency bands identified in the BCP powders are described as follows [23, 24, 29]. Small vibrational bands are perceived around 3420 and 1646  $\text{cm}^{-1}$ , indicating the binding mode of the adsorbed water. The small vibrational band observed around 2365  $\text{cm}^{-1}$  is characteristic of the presence of free  $\text{CO}_2$ . Vibrational bands related to the  $\text{PO}_4^{3-}$  asymmetric stretching mode are observed around 960, 1019, 1056, 1107, and 1210  $\text{cm}^{-1}$ . The vibrational bands around 720 and 890  $\text{cm}^{-1}$  indicated the asymmetric stretching and corresponding broadening of the C-O bond of the  $\text{CO}_3^{2-}$  groups existing in the phosphate crystallographic lattice. The vibrational bands

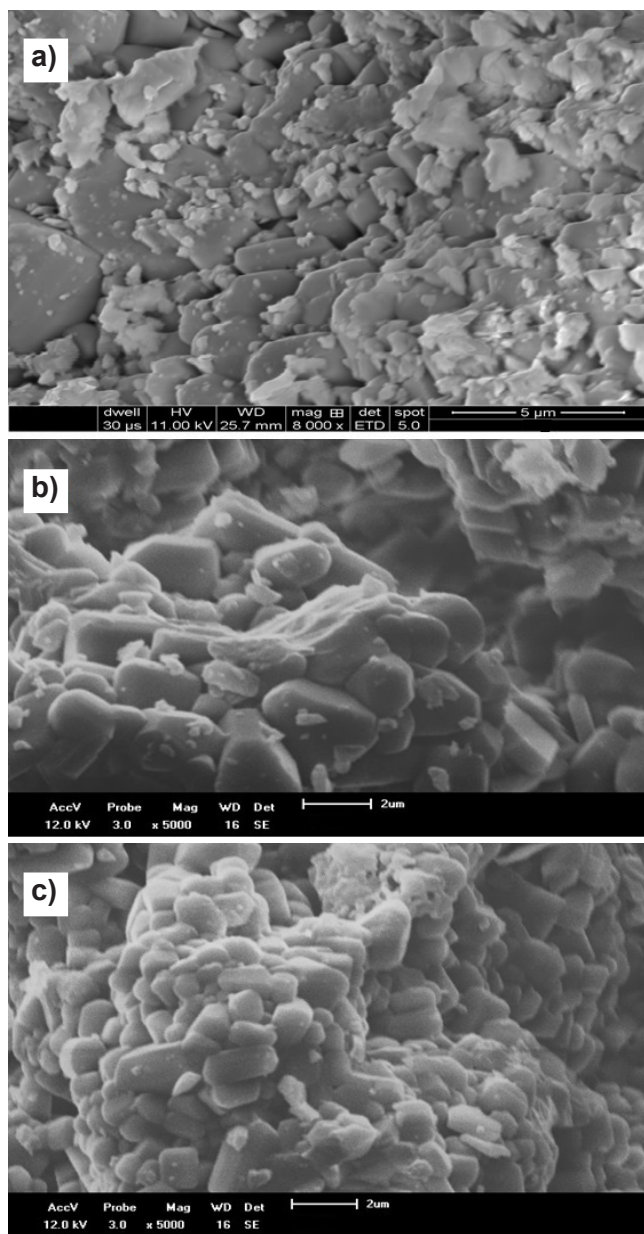


Figure 5: SEM micrographs showing the morphology of the as-synthesized BCP powders: a) BTC1; b) BTC2; and c) BTC3.

Table III - Ca and P contents and Ca/P ratio values of the synthesized BCP powders.

Sample	Ca (at%)	P (at%)	Ca/P
BTC1	20.80	13.29	1.56
BTC2	30.80	24.02	1.28
BTC3	31.10	24.02	1.29

found around 450, 490, 563, and 620  $\text{cm}^{-1}$  can be attributed to asymmetric stretching and/or deformation of O-P-O in  $\text{PO}_4^{3-}$ . However, the vibrational bands found around 720  $\text{cm}^{-1}$  and in the range of 500-580  $\text{cm}^{-1}$  range could also be related to Ca ions. Indeed, the synthesized BCP powders contained a small amount of residual Ca ions, as shown in Fig. 3 and Table I.

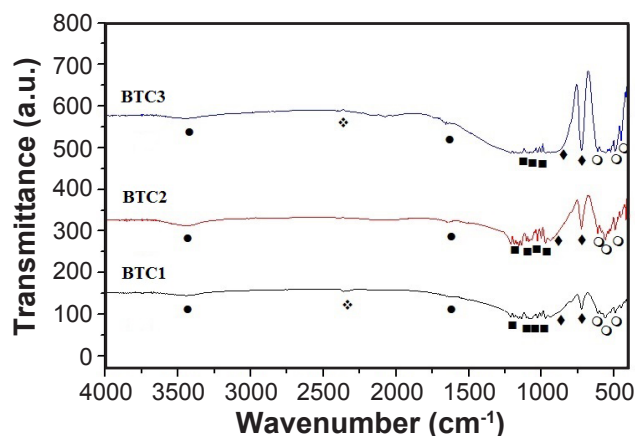


Figure 6: FTIR spectra of the synthesized BCP powders: ●  $\text{H}_2\text{O}$ ; ❖  $\text{CO}_2$ ; ■  $\text{PO}_4^{3-}$ ; ◆  $\text{CO}_3^{2-}$ ; and ○  $\text{PO}_4^{3-}$ .

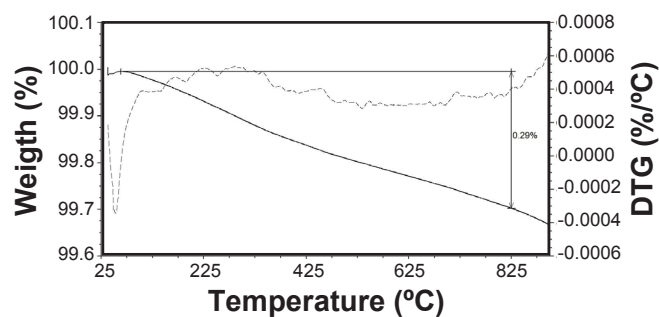


Figure 7: TG/DTG curves of the BTC1 sample.

Table IV - Mass loss (wt%) of the BCP powders during heating up to 900 °C.

BTC1	BTC2	BTC3
0.29	0.40	0.38

Thermogravimetric analysis (TG/DTG) was used to determine the thermal stability of the new BCP powders during heating. An example of TG/DTG curves for the BTC1 sample is shown in Fig. 7. The total mass losses between 25 e 900 °C for the synthesized BCP powders are summarized in Table IV. Low mass loss values between 0.29% and 0.40% were found, which can be attributed to the elimination of physically adsorbed water. Thus, the BCP powders derived from tilapia carcass waste obtained in this work were highly stable when exposed to relatively high temperatures of up to 900 °C. This result could be highly relevant in terms of potential practical application in the medical field.

## CONCLUSIONS

Nanostructured biphasic calcium phosphate, BCP [ $\beta$ -calcium pyrophosphate ( $\beta$ -CPP)/ $\beta$ -tricalcium phosphate ( $\beta$ -TCP)], powders were successfully synthesized by the simple wet precipitation method using tilapia carcass waste as a sustainable calcium precursor. It was found by XRD

analysis and Rietveld refinement that the BCP powders were a  $\beta$ -CPP/ $\beta$ -TCP mixture with a higher amount of  $\beta$ -CPP, depending on the  $\text{HNO}_3$  concentration. The effect of the  $\text{HNO}_3$  concentration was to increase the amount of the  $\beta$ -CPP phase. The BCP powders had an average crystallite size in the range of 57.7-59.4 nm, smooth plate morphology, and were highly agglomerated. FTIR analysis confirmed the typical vibrational bands of calcium phosphate materials. The TG/DTG analyses suggested the high thermal stability of the synthesized BCP powders. Thus, the development of new nanostructured BCP powders derived from tilapia carcass waste can be of high interest for biomedical applications, but at the same time, it also helps to preserve the environment in a friendly way.

#### ACKNOWLEDGMENTS

This study was financed in part by the National Council for Scientific and Technological Development - Brazil (CNPq) - Process No. 307507/2019-0 and the Foundation for Research Support of the State of Rio de Janeiro - Brazil (FAPERJ) - Process No. E-26/201.137/2022. The authors also would like to thank Teresa Eligio Castillo (SEPOL/LAMAV/UENF) for her support in thermal analysis.

#### REFERENCES

- [1] M.L.R. Souza, L.C. Godoy, J.V. Visentainer, N.E. Souza, N.P. Franco, G.G. Oliveira, A.C. Feihmann, E.S.R. Goes, *Res. Soc. Develop.* **10**, 16 (2021) e583101621134.
- [2] Associação Brasileira da Piscicultura, *Anuário Brasileiro da Piscicultura 2023*, São Paulo (2023).
- [3] M.H. Leira, A.F. Nascimento, F.R. Alves, L. Orfao, Y.G. Lacerda, H.A. Botelho, L. Reghim, A.A. Lago, *Food Sci. Technol.* **39**, Suppl. 1 (2019) 63.
- [4] E.S. Reis, S. Cardoso, T.E. Oliveira, *Res. Soc. Develop.* **12**, 1 (2023) e27812135831.
- [5] W. Habraken, P. Habibovic, M. Epple, M. Bohner, *Mater. Today* **19**, 2 (2016) 69.
- [6] N. Eliaz, N. Metoki, *Materials* **10**, 334 (2017) 1.
- [7] T. Safronova, V. Putlayev, Y. Filippov, T. Shatalova, E. Karpushkin, D. Larionov, G. Kazakova, Y. Shakhtarin, *Ceramics* **1** (2018) 375.
- [8] S.R. Vasant, M.J. Joshi, *Rev. Adv. Mater. Sci.* **48** (2017) 44.
- [9] T.V. Safronova, V.I. Putlayev, K.A. Bessonov, V.K. Ivanov, *Proc. Appl. Ceram.* **7** (2013) 9.
- [10] S.E. Lobo, T.L. Arinze, *Materials* **3** (2010) 815.
- [11] S.V. Dorozhkin, *Ceram. Int.* **42**, 6 (2016) 6529.
- [12] J.M. Bouler, P. Pilet, O. Gauthier, E. Verron, *Acta Biomater.* **53** (2017) 1.
- [13] N.F. Mohammad, K.L. Mei, M.R.M. Roslan, S.S.M. Saleh, F.D.M. Daud, *J. Phys. Conf. Ser.* **2071** (2021) 12009.
- [14] J.N.F. Holanda, in "Handbook of ecomaterials", L.M.T. Martínez, O. Kharissova, B. Kharisov (Eds.), Springer, Cham (2019) 2371.
- [15] A. Pal, S. Paul, A.R. Choudhury, V.K. Balla, M. Das, A. Sinha, *Mater. Lett.* **203** (2017) 89.
- [16] P. Terzioğlu, H. Öğüt, A. Kalemtaş, *Mater. Sci. Eng. C Mater. Biol. Appl.* **91** (2018) 899.
- [17] A.F.A. Latif, N.A.S. Mohd Pu'ad, N.A.A. Ramli, M.S. Muhamad, H.Z. Abdullah, M.I. Idris, T.C. Lee, *Mater. Sci. Forum* **1010** (2020) 584.
- [18] M. Bas, S. Daglilar, N. Kuskonmaz, C. Kalkandelen, G. Erdemir, S.E. Kuruca, D. Tulyaganov, T. Yoshioka, O. Gunduz, D. Fikai, A. Fikai, *Int. J. Mol. Sci.* **21** (2020) 8082.
- [19] H.B. Modolon, J. Inocente, A.M. Bernardin, O.R.K. Montedo, S. Arcaro, *Ceram. Int.* **47**, 19 (2021) 27685.
- [20] S.K. Dermawan, Z.M.M. Ismail, M.Z. Jaffri, H.Z. Abdullah, *J. Phys. Conf. Ser.* **2169** (2022) 12034.
- [21] S. Belouafa, A. Bennemara, A. Abourriche, *Curr. Trends Biomed. Eng. Biosci.* **6**, 3 (2017) 555690.
- [22] N.D. Montañez, H.A. Estupiñanb, S.J. García, D.Y. Peña, *Chem. Eng. Transac.* **64** (2018) 307.
- [23] T.H.A. Corrêa, J.N.F. Holanda, *Mat. Res.* **22**, Suppl. 1 (2019) e20190486.
- [24] T.H.A. Corrêa, J.N.F. Holanda, *Trends Phys. Chem.* **17** (2017) 75.
- [25] D.L. Bish, S.A. Howard, *J. Appl. Crystal.* **21** (1998) 86.
- [26] M. Tamer, *J. Mod. Phys.* **4** (2013) 1149.
- [27] O. Bokuniaeva, A.S. Vorokh, *J. Phys. Conf. Ser.* **1410** (2019) 12057.
- [28] K. Venkateswarlu, M. Sandhyarani, T.A. Nellaippan, N. Rameshbabu, *Procedia Mater. Sci.* **5** (2014) 212.
- [29] M. Ebrahimi, M.G. Botelho, S.V. Dorozhkin, *Mater. Sci. Eng. C* **71** (2017) 1293.

(Rec. 22/06/2023, Ac. 14/09/2023)

